

# Selecting and Scaling of Real Accelerograms

**B.Ö. Ay & S. Akkar**

*Earthquake Engineering Research Center, Department of Civil Engineering,  
Middle East Technical University, Turkey*



## ABSTRACT

Ground motion selection and scaling methodologies are evaluated to obtain suitable sets of records that represent a pre-defined seismic level with low dispersion in structural response. As part of this objective, we focused on reducing the scatter in structural response by scaling ground motions through the estimations obtained from ground-motion prediction equations (GMPEs). This way the fundamental geophysical features of the records are preserved. The GMPEs are employed for different intensity parameters (spectral and peak ground motions) and dispersion statistics of nonlinear single-degree-of-freedom (SDOF) response are calculated for most efficient intensity parameter in ground-motion scaling in view of the variations in magnitude and distance.

*Keywords: Dispersion in structural response, ground-motion prediction equation, efficient intensity parameter*

## 1. INTRODUCTION

Scaling of accelerograms is necessary to establish suits of actual strong motions to estimate structural response accurately for a target hazard. This way, the analyst can reduce the number of ground motions required to obtain reliable information on the seismic performance of structural systems. Scaling of accelerograms is also used to investigate different structural response states as in the case of incremental dynamic analysis.

The objective of this study is to investigate 2 scaling techniques for modifying accelerograms for target hazard levels. The first method, (Method 1) fulfils this objective by using the estimations of GMPEs that account for the specific features (moment magnitude, site class) of the ground motion. The second procedure (Method 2) establishes a scaling strategy on the median ground motion of a particular suit of records. These two methodologies are compared in terms of dispersion statistics of structural response obtained from elastic, constant strength, and constant base shear analyses. Efficiency of using peak ground motion parameters (PGA and PGV) as alternatives to scaling via spectral ordinates and sensitivity of Method 1 to the variations in magnitude and distance intervals from which the records are selected are also scrutinized in this study.

## 2. GROUND MOTION SELECTION

Record selection is based on the reliability and consistency of data processing, as well as the uniformity of records in terms of magnitude and distance metrics. The recently compiled Turkish strong-motion database<sup>1</sup> is used as the main source whereas for a better magnitude-distance distribution, additional ground motion records are gathered from PEER (<http://peer.berkeley.edu/nga>) and European strong-motion databank (Ambraseys et al., 2004). Records that satisfy NEHRP C and D

---

<sup>1</sup> The Turkish strong-motion database is compiled under the project entitled "Compilation of Turkish strong-motion network according to the international standards" with an award no. 105G016 granted by The Scientific and Technological Research Council of Turkey.

site classifications (BSSC, 2003) are selected and then clustered for specific moment magnitude ( $M_w$ ) and  $R_{jb}$  (closest distance between station and horizontal surface projection of fault rupture) intervals. The entire database is divided into 9 ground-motion bins that are composed of 3 magnitude [small magnitude, SM, ( $5.0 \leq M_w < 6.0$ ), intermediate magnitude, IM, ( $6.0 \leq M_w < 6.5$ ) and large magnitude, LM, ( $6.5 \leq M_w < 7.6$ )] and 3 distance [short distance, SR, ( $0 \text{ km} \leq R_{jb} < 20 \text{ km}$ ), intermediate distance, IR, ( $20 \text{ km} \leq R_{jb} < 50 \text{ km}$ ) and large distance, LR, ( $50 \text{ km} \leq R_{jb} < 100 \text{ km}$ )] intervals.

As part of ground-motion selection process, a statistical analysis is conducted to exclude the outlier records in order to ensure the spectral shape compatibility within the strong-motion bins that is defined as one of the important factors in reducing the variability in structural response (Bommer and Acevedo, 2004; Baker and Cornell, 2005; Baker and Cornell, 2006; Luco and Bazzurro, 2007). Elastic spectral ordinates of accelerograms in each  $M_w$ - $R_{jb}$  bin are compared with the corresponding bin average for the specific periods considered in this study (i.e.  $T=0.3\text{s}$ ,  $0.6\text{s}$ ,  $0.9\text{s}$ ,  $1.2\text{s}$ , and  $1.5\text{s}$ ). Accelerograms having spectral ordinate values outside the mean  $\pm 2$  standard deviation bandwidth are accepted as outliers and they are removed from the database.

### 3. INVESTIGATED SCALING METHODOLOGIES

#### 3.1. Scaling with respect to a Predefined GMPE

Method 1 constrains the scaling to the estimations of GMPEs. Ground-motion records are scaled considering their actual seismological parameters (i.e. magnitude, distance and site class) and scaling factor is computed from the difference between the actual ground motion and its estimation from a representative GMPE. This is, in a way, utilization of epsilon ( $\epsilon$ ) concept (Baker and Cornell, 2005; Baker and Cornell, 2006) in ground-motion scaling. We selected the Akkar and Bommer (2007a) (hereinafter AB07) model as our GMPE and analysis results are derived in terms of spectral displacement (SD) because this model estimates SD. [Note: Any spectral quantity (pseudo-spectral acceleration, pseudo-spectral velocity and spectral displacement) or peak ground motion values (PGA and PGV) can be implemented in Method 1.] The model predicts for the geometric mean of SD ordinates, hence a single scaling factor for each accelerogram is found using the two horizontal components. The same scaling factor is then applied to both horizontal components simultaneously to preserve the original difference between these components (Bommer and Acevedo, 2004). The mathematical expressions that describe the computation of scaling factor are presented in Equations 3.1 to 3.3. Given the magnitude, site and distance properties of a particular accelerogram, Eqn. 3.1 describes the calculation of epsilon ( $\epsilon$ ) where  $\log_{10}(\text{SD}(T_i, \xi)_{\text{rec}})$  is the logarithm of the geometric mean of spectral quantity of the record and  $\log_{10}(\text{SD}(T_i, \xi)_{\text{GMPE,median}})$  is the logarithm of the GMPE estimate at period ( $T_i$ ) and damping ( $\xi$ ). The parameter  $\sigma(T_i, \xi)$  is the standard deviation of the considered GMPE at  $T_i$  and  $\xi$ .

The target SD for a scenario earthquake,  $\text{SD}(T_i, \xi)_{\text{target}}$ , is obtained in Eqn. 3.2 by modifying the median SD estimation of GMPE for the scenario event (i.e.  $\text{SD}(T_i, \xi)_{\text{GMPE,target}}$ ) using the epsilon computed in Eqn. 3.1. This way, the inherent aleatory variability of ground motions is considered. The major assumption in Eqn. 3.2 is the independency of  $\sigma$  with the variations between the actual  $M_w$ - $R_{jb}$  pair of the record and the target  $M_w$ - $R_{jb}$  pair of the scenario event. In this study, the average magnitude value of the records in each ground-motion bin represents the target  $M_w$  of the scenario event. The  $R_{jb}$  distances for scenario events are selected as 10 km, 35 km, and 75 km for SR, IR and LR distance intervals, respectively. Other seismological parameters (site class and fault mechanism) used for computing the target spectral quantity are taken as those of the actual record. The scaling factor of each accelerogram is found as given in Eqn. 3.3 by computing the ratio between the target and actual SD. This factor is applied to the horizontal components of the accelerogram simultaneously to preserve the original difference between each other.

$$\epsilon(T_i, \xi) = \frac{\log_{10}(\text{SD}(T_i, \xi)_{\text{rec}}) - \log_{10}(\text{SD}(T_i, \xi)_{\text{GMPE,median}})}{\sigma(T_i, \xi)} \quad (3.1)$$

$$SD(T_i, \xi)_{\text{target}} = SD(T_i, \xi)_{\text{GMPE, target}} \times 10^{\epsilon\sigma} \quad (3.2)$$

$$\text{ScalingFactor} = \frac{SD(T_i, \xi)_{\text{target}}}{SD(T_i, \xi)_{\text{rec}}} \quad (3.3)$$

Fig. 3.1 illustrates a scaling example for NEHRP C accelerogram of  $M_w=5.9$  and  $R_{jb}=4$  km (SM-SR bin). The target scenario is represented by an event with  $M_w=5.4$  and  $R_{jb}=10$  km. The scaling is performed for a 5%-damped SD at  $T_i=0.6$ s. The geometric mean SD of the real accelerogram ( $SD_{\text{rec}}$ ) is computed and the corresponding estimation from the considered GMPE ( $SD_{\text{AB07, median}}$ ) is obtained using the seismological parameters of the record. Afterwards, epsilon is calculated as described in Eqn. 3.1. The estimation of GMPE for target scenario ( $SD_{\text{AB07, target}}$ ) is modified by using the computed epsilon to obtain the target spectral displacement ( $SD_{\text{target}}$ ). In the final step, the ratio of  $SD_{\text{target}}$  to  $SD_{\text{rec}}$  is used to scale each horizontal component of the real accelerogram.

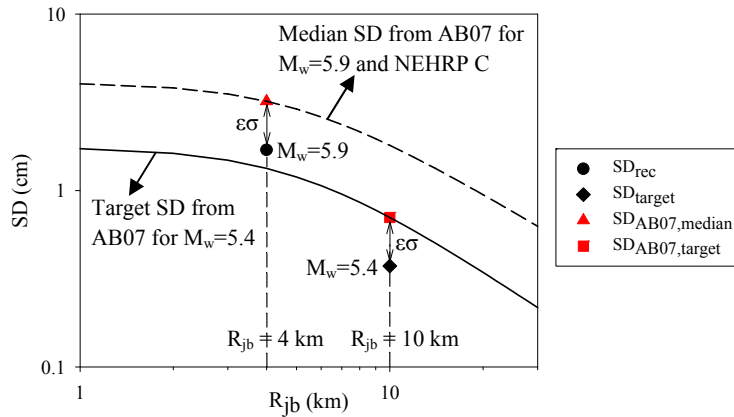


**Figure 3.1.** A scaling example for Method 1

### 3.2. Scaling to a Target Average Value of a Ground-Motion Bin

The method is proposed by Shome et al. (1998) and it is a widely accepted scaling methodology in the engineering community as it focuses on the concepts that are familiar to the structural engineers. Shome et al. (1998) pointed out that the number of records required to obtain an estimate of the median response depends on the standard deviation of the analysis results and proposed to scale each record in a ground motion ensemble to the median spectral ordinate of the bin (at a given period) in order to reduce dispersion in dynamic response. Shome et al. (1998) concluded that such a scaling procedure produces unbiased nonlinear response results. In this study Method 2 is implemented such that each record within a ground motion bin (LM-SR, SM-LR, etc.) is scaled individually to the bin-median spectral acceleration at the predetermined vibration periods.

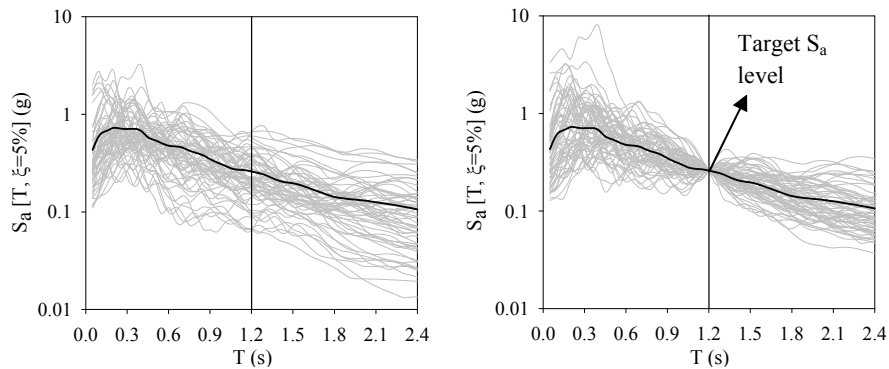


**Figure 3.2.** Scaling to the bin-median spectral acceleration according to Method 2. Black line is presenting the average acceleration spectrum of LM-SR bin.

Fig. 3.2 shows acceleration spectra of the recordings in LM-SR bin before (left) and after (right) scaling using Method 2 for  $T=1.2s$ . Note that, Method 1 considers the standard deviation of GMPEs to address the aleatory variability whereas the ground-motion variability in Method 2 is limited to the variations of records in the considered ground-motion bin. Since GMPEs are based on much larger datasets, the aleatory variability described by their standard deviation is more definite with respect to the one described through Method 2.

#### 4. EFFECT OF SCALING ON DISPERSION

Scaling methodologies that are described above are investigated in terms of dispersion and the level of manipulation of the real accelerograms. This study is based on three major evaluation levels. In the first level, Methods 1 and 2 are compared via COV statistics and the amplitude of scaling.

Spectral analyses of SDOF systems are conducted to compare the efficiency of the scaling methods in reducing the scatter in structural response. SDOF analysis is preferred in this study, for comparisons of scaling methodologies, in order to exclude the variability that can originate from structural modelling uncertainties. The nonlinear response of SDOF systems is represented by bilinear hysteretic model with 3% post-yield stiffness. Although scaling procedure of Method 1 is based on the geometric mean of two horizontal components, for consistency with Method 2, each scaled accelerogram component in a ground-motion bin is included in the comparative statistics. The results are described for elastic, constant strength ( $R$ , elastic strength normalized by the yield strength of the SDOF system) and constant base shear spectral displacements for  $T=0.3s, 0.6s, 0.9s, 1.2s,$  and  $1.5s$ .

Fig. 4.1 compares the COV statistics of Method 1 (left panel) and Method 2 (right panel) for the entire set of  $M_w-R_{jb}$  bins considered in this study. The figures depict that COV statistics of Method 2 increases with the increasing level of inelasticity (represented by the increase in  $R$ ). The COV statistics of Method 1 displays a more stable trend with respect to Method 2 suggesting that the uncertainty in nonlinear structural response is influenced less with the variations in the inelasticity level for this scaling methodology. Inherent to the scaling strategy of Method 2, the COV is 0 for the elastic case.

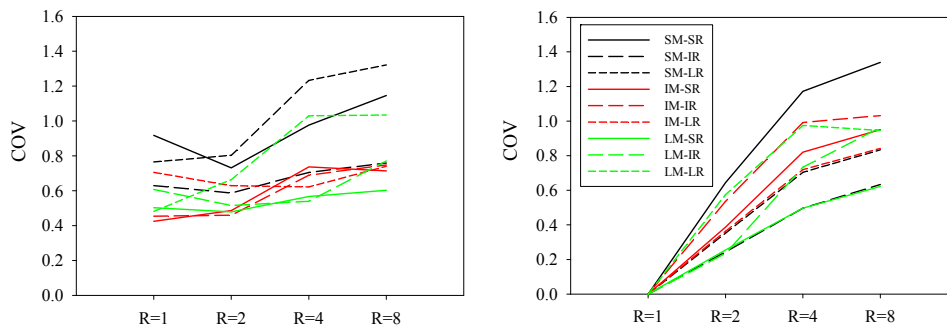


**Figure 4.1.** COV statistics computed at  $T=0.6s$  for constant strength values varying between  $R=1$  (elastic behaviour) and  $R=8$  (highly nonlinear behaviour)

Fig. 4.2 explores the discussions in Fig. 4.1 in a more specific way. It compares the dispersion statistics of Method 1 and Method 2 for two particular  $R$  values and one constant base shear value as a function of vibration periods considered in this study. The panel on the left compares COV statistics for a moderate level inelasticity whereas the middle panel exhibits the same statistics for  $R=8$  (high level inelasticity). Right-hand-side panel shows COV statistics for  $\text{ETA}=0.1$ . The comparative plots show that Method 2 results in high dispersion in short period structural response and dispersion increases with increasing inelasticity level. In fact, the dispersion in Method 1 is almost insensitive to the changes in the level of inelasticity whereas scatter (COV) increases considerably in Method 2 when normalized lateral strength changes from  $R=4$  to  $R=8$ . Scaling of records to bin-median ground motion at a particular elastic period and inherent period shift with increasing level of inelasticity is the

most reasonable explanation of amplified dispersion in Method 2 as inelasticity attains larger levels. Since the period elongation is much more pronounced at short-period structural systems, the uncertainty in structural response is much higher in Method 2 when compared to Method 1.

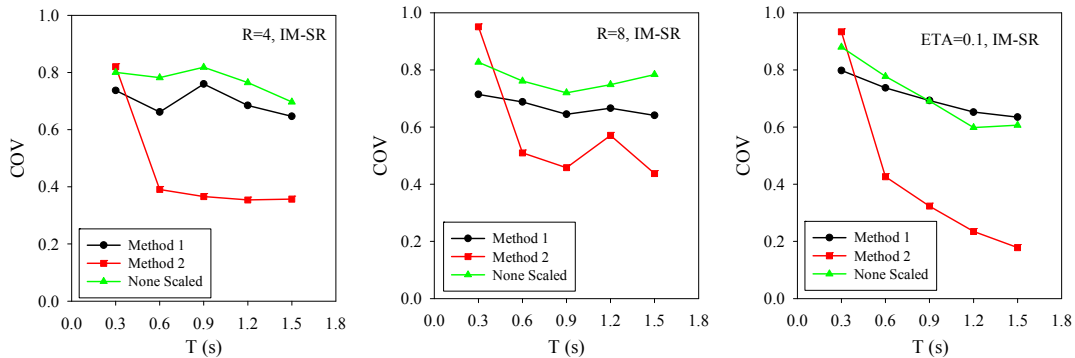


**Figure 4.2.** COV statistics of SDOF systems as a function of period with different level of inelasticity

The level of scaling of accelerograms has been the subject of discussion by many researchers. Luco and Bazzurro (2007) concluded that large scaling factors can introduce a systematic bias to the median nonlinear structural response that tends to increase with decreasing strength and structural period. Iervolino and Cornell (2005) stated that scaling factors up to 4 do not introduce significant bias to the nonlinear peak displacements of moderate to short period SDOF systems. Based on these discussions one would immediately infer that records that are scaled with factors close to 1 are not manipulated significantly (i.e. they still preserve their fundamental seismological features after being scaled) and would yield relatively more reliable results in terms of structural response. Bearing on these discussions Fig. 4.3 presents the maximum and minimum scaling factors used by Method 1 and Method 2. The plots clearly show that scaling factors of Method 2 are significantly larger than those of Method 1. While the maximum amplification factors of Method 1 vary between 2 and 4, the maximum scaling values of Method 2 are generally above 10 and reach to values of 20 that would suggest a significant manipulation in the genuine features of the ground motions.

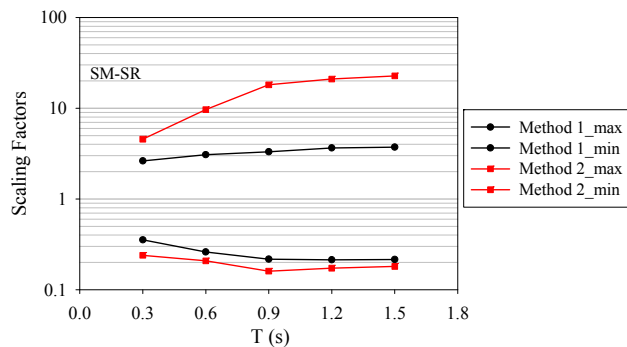
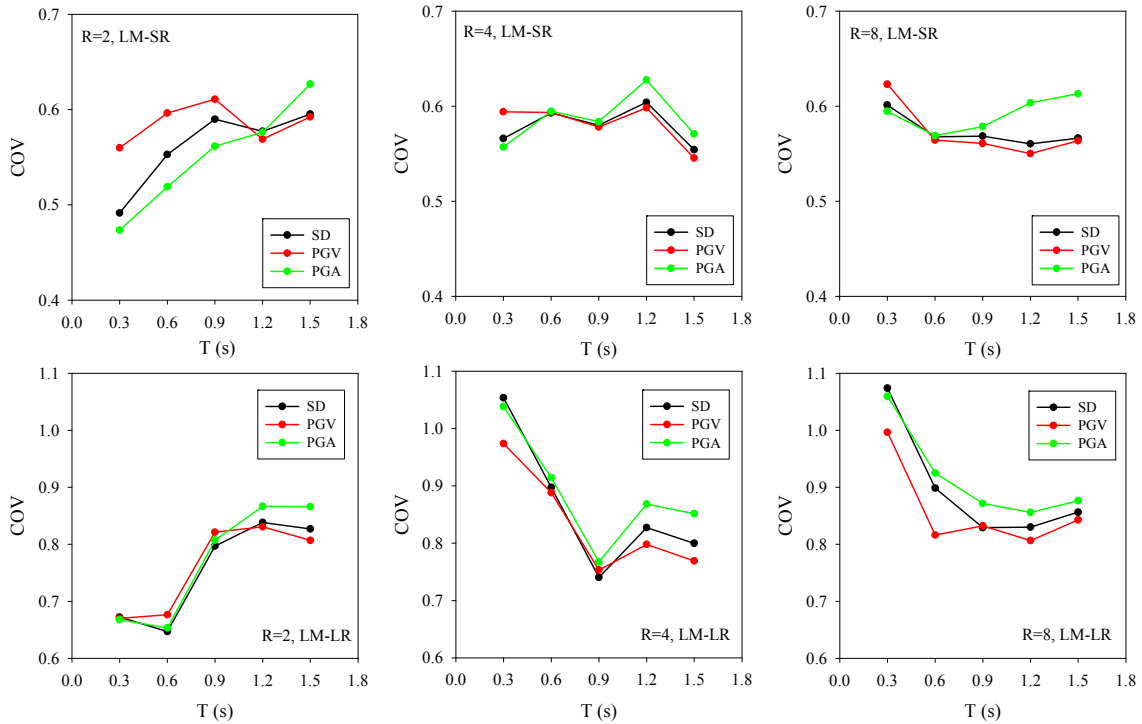


**Figure 4.3.** COV results and corresponding maximum scaling factors used by Methods 1 and 2

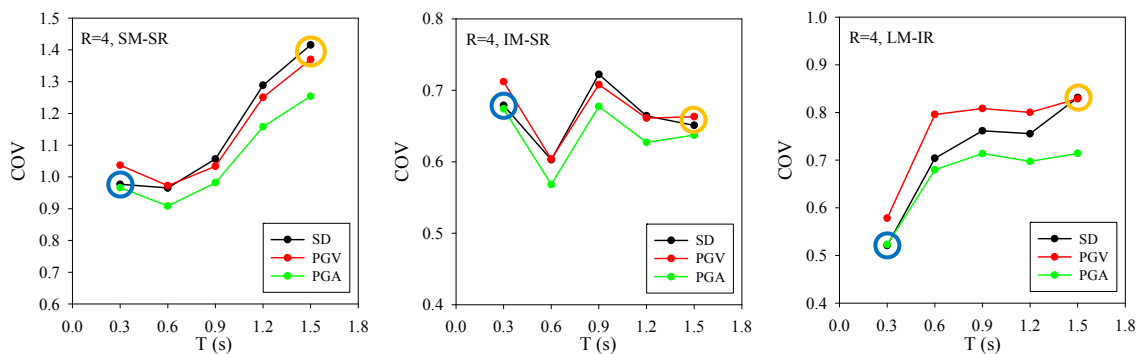
In the second level evaluation, we investigated the efficiency of implementing peak ground motion parameters (PGA and PGV) in Method 1 as alternative intensity measures to SD. As stated previously, although the prediction equation proposed by Akkar and Bommer (2007a) estimates SD, equations developed to predict other intensity measures can also be implemented in Method 1. Accordingly, GMPEs presented by Akkar and Bommer (2007a) and Akkar and Bommer (2007b) are employed in Method 1 to estimate PGA and PGV respectively.

Fig. 4.4 compares the COV statistics of Method 1 for PGA, PGV and SD. For LM-SR and LM-LR bins target magnitude ( $M_w$ ) value is taken as 7.0 and 7.1, whereas target distance ( $R_{jb}$ ) values are taken as 10 km and 75 km, respectively. The figures depict that scaling with respect to PGA results in relatively high dispersion as inelasticity attains larger levels (third column). Similar relationship is also

observed for long-period systems. For moderate inelasticity levels, there is almost no difference between COV results of systems having moderate vibration periods. Fig. 4.4 also shows that scaling with respect to PGV results in relatively high dispersion for short period systems at low inelasticity levels. The dispersion becomes low at longer period systems with high inelasticity levels for PGV scaling. Similar results were also obtained by Akkar and Özen (2005) that investigated the effect of PGV on deformation demands for SDOF systems. Fig. 4.5 compares the dispersions resulting from PGA, PGV and SD based scaling. Note the comparable dispersion between PGA and SD scaling at low periods ( $T=0.3s$ ). In a similar fashion, PGV and SD based scaling are in good agreement for high periods ( $T=1.5s$ ). We note that the scatter of PGA, PGV and SD used in scaling also influences the variations of nonlinear oscillator response. This is not discussed in text due to space limitations.



**Figure 4.4.** Comparison of PGA with PGV and SD for different inelasticity levels and periods



**Figure 4.5.** COV comparisons between PGA, PGV and SD based scaling for inelastic spectra of  $R=4$

Another important aspect of scaling real accelerograms is the sensitivity to the variations in magnitude and distance intervals from which the records are selected. To test this sensitivity additional sets of analysis are conducted by modified ground-motion bins for different M-R boundaries. Two types of ground-motion bins are developed. First type is assembled to test the dependency of results on the magnitude. Accordingly, previous  $R_{jb}$  intervals are kept same and two magnitude groups (e.g. SM and IM) are combined. Second type gathered to test the sensitivity of results to the  $R_{jb}$  distance. For this case, magnitude bins are kept the same and two  $R_{jb}$  intervals (e.g. SR and IR) are combined.

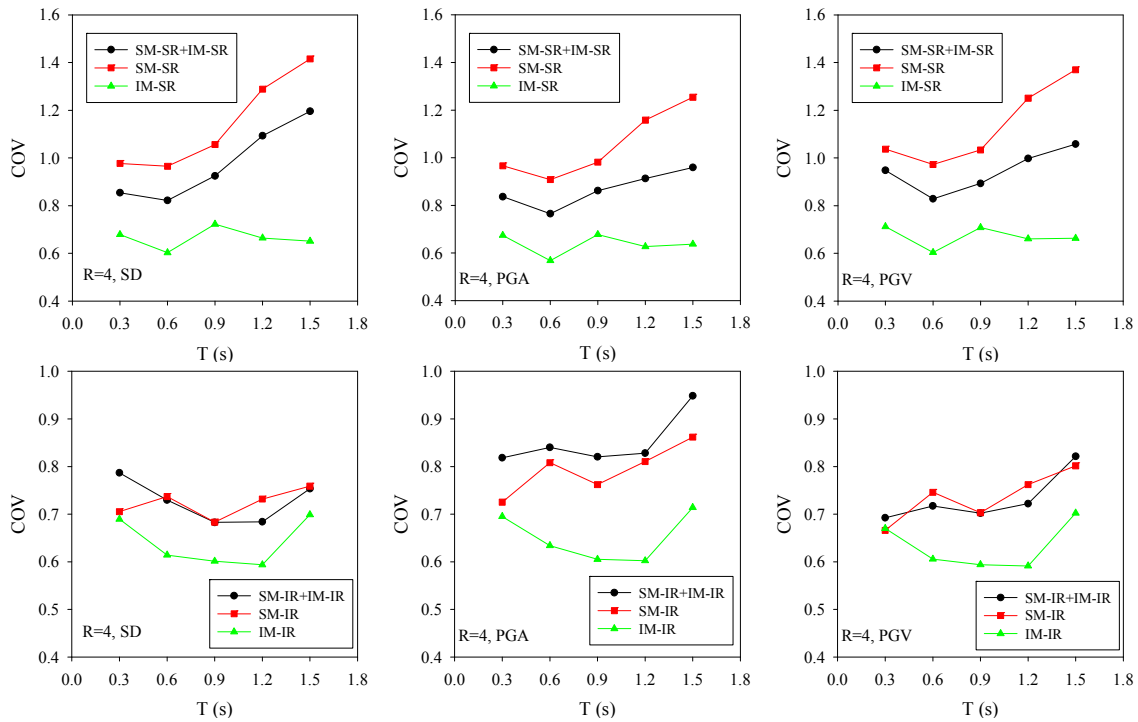


**Figure 4.6.** The effect of magnitude interval on COV statistics of scaled records

Fig. 4.6 presents the sensitivity of COV statistics to magnitude intervals. The new bins are assembled from SM-SR and LM-SR (upper row plots) and SM-IR and IM-IR (lower row plots) ground-motion bins. The dispersion statistics given in Fig. 4.6 show that the effect of the magnitude on the dynamic response scatter is significant. Therefore, it can be recommended that the selection of records should be based on narrow magnitude intervals with an average value equal to the scenario event. This criterion is quantified as 0.25 and 0.2 units either side of the target value by Stewart et al. (2001) and Bommer and Acevedo (2004), respectively.

Fig. 4.7 shows the effect of distance interval on COV statistics. The plots compare combined LM-SR+LM-IR ground-motion bin with the LM-SR and LM-IR bins. The figure depicts that Method 1 scaling is less sensitive to distance than to magnitude. Accordingly, the distance boundaries can be relaxed if it is required to increase the number of records.

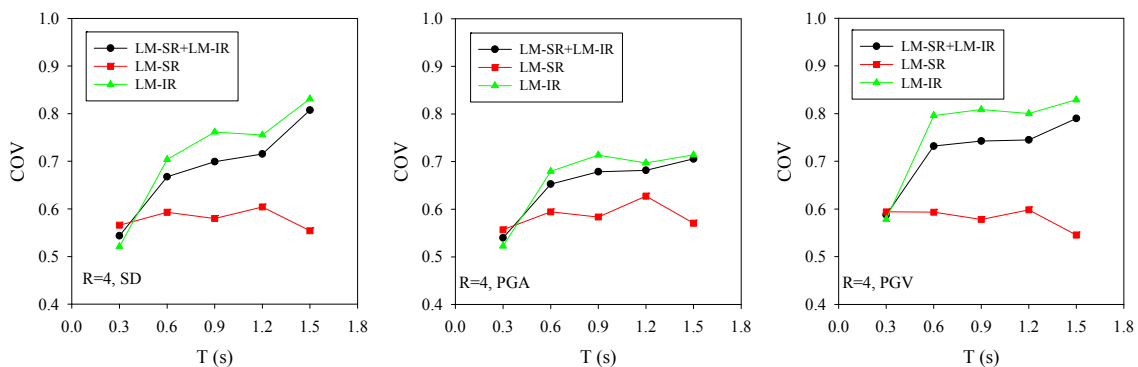


**Figure 4.7.** The effect of source-to-site distance interval on COV statistics of scaled records

## 5. SUMMARY AND CONCLUSION

Selection and scaling of real accelerograms are investigated in terms of dispersion in nonlinear response and the level of manipulation of records. Accelerograms having reliable seismological

parameters (magnitude, site class, faulting style and source-to-site distance) are first selected, re-evaluated using a simple outlier analysis and then grouped for different magnitude and distance intervals.

Two different scaling procedures are studied using the assembled dataset. The first method (Method 1) that is based on the predictive model estimations results in lower dispersion in short-period nonlinear SDOF response at moderate or high inelasticity levels. The second method (Method 2) scales the ground motions to the median spectral ordinate of the ground-motion bin and it yields lower dispersion with the increase in oscillator's vibration period. Scaling factors used in Method 2 are significantly higher or lower than those of Method 1 and this may indicate a considerable manipulation of records by Method 2.

The efficiency of implementing PGA or PGV based ground-motion scaling is also investigated. PGA scaling results in lower dispersion in nonlinear SDOF response at short periods when the level of inelasticity is moderate or low. As the inelasticity level increases and period attains larger values, lower dispersion is achieved by PGV based scaling. Finally, the sensitivity of scaling to variations in magnitude and distance suggests that in ground-motion binning, provided an initial outlier analysis, narrow magnitude intervals and more relaxed distance ranges are efficient for reducing the dispersion in nonlinear structural response before scaling.

#### ACKNOWLEDGEMENT

This study is conducted as part of the project entitled "A probability based seismic loss model concerning the common concrete buildings in Turkey" that is funded by ODTU-BAP under the award No. BAP-03-03-2009-04. The authors also acknowledge the project entitled "Compilation of Turkish strong-motion network according to the international standards" that provided most of the ground motions used in this study. This project is granted by The Scientific and Technological Research Council of Turkey under the award no. 105G016.

#### REFERENCES

- Akkar, S. and J. J. Bommer, (2007a). Prediction of Elastic Displacement Response Spectra in Europe and the Middle East. *Earthquake Engineering and Structural Dynamics*. **36**, 1275–1301.
- Akkar, S. and J.J. Bommer (2007b). Empirical prediction equations for peak ground velocity derived from strong-motion records from Europe and the Middle East. *Bulletin of the Seismological Society of America*. **97:2**, 511–530.
- Akkar, S. and Ö. Özen (2005). Effect of peak ground velocity on deformation demands for SDOF systems. *Earthquake Engineering and Structural Dynamics*. **34:13**, 1551–1571.
- Ambraseys, N. N., P. Smit, J. Douglas, B. Margaris, R. Sigbjörnsson, S. Olafsson, P. Suhadolc and G. Costa (2004). Internet site for European strong-motion data. *Bollettino di Geofisica Teorica ed Applicata*. **45:3**, 113–129.
- Baker J. W. and C. A. Cornell, (2005). A vector-valued ground motion intensity measure consisting of spectral acceleration and Epsilon. *Earthquake Engineering and Structural Dynamics*. **34:10**, 1193–1217.
- Baker J. W. and C. A. Cornell, (2006). Spectral shape, epsilon and record selection, *Earthquake Engineering and Structural Dynamics* **35**, 1077–1095.
- Building Seismic Safety Council (BSSC), (2003). NEHRP recommended provisions for seismic regulations for new buildings and other structures. Rep. FEMA-450, Washington, D.C.
- Bommer J. J. and A. B. Acevedo, (2004). The Use of Real Earthquake Accelerograms as Input to Dynamic Analysis. *Journal of Earthquake Engineering*. **8:Special Issue 1**, 43–91.
- Iervolino I. and C. A. Cornell, (2005). Record selection for nonlinear seismic analysis of structures *Earthquake Spectra* **21 (3)**, 685–713.
- Luco N. and P. Bazzurro, (2007). Does amplitude scaling of ground motion records result in biased nonlinear structural drift responses? *Earthquake Engineering and Structural Dynamics*. **36:13**, 1813–1835.
- Shome, N., C. A. Cornell, P. Bazzurro, and J. E. Carballo, (1998). Earthquakes, records and nonlinear responses. *Earthquake Spectra*. **14:3**, 469–500.
- Stewart, J. P., S. J. Chiou, J. D. Bray, R. W. Graves, P. G. Somerville, and N. A. Abrahamson, (2001). Ground motion evaluation procedures for performance-based design. PEER Report 2001/09, Pacific Earthquake Engineering Research Center, University of California, Berkeley.